Polarization states and coherent effects in a coherently pumped $J''=1 \rightarrow J=0 \rightarrow J'=1$ isotropic-cavity laser

A. Kul'minskii,[1,*] R. Vilaseca,[1] R. Corbalán,[2] and N. Abraham[3]

[1]*Departament de Física i E. N., Universitat Politécnica de Catalunya, Colom 11, E-08222 Terrassa, Barcelona, Spain*
[2]*Departament de Física, Universitat Autònoma de Barcelona, E-08193 Bellaterra, Spain*
[3]*Physics Department, DePauw University, Greencastle, Indiana 46135-0037*

We have theoretically explored the behavior of a coherently pumped $J''=1 \rightarrow J=0 \rightarrow J'=1$ isotropic cavity laser and compared it with the behavior of other related laser systems involving atomic or molecular levels with angular quantum numbers 0 and 1. It is shown that at low and moderate pumping strengths it behaves very differently from the $J''=0 \rightarrow J=1 \rightarrow J'=0$ laser exhibiting no pump-induced gain anisotropy and allowing for linearly polarized (LP) solutions with arbitrary azimuth and circularly polarized (CP) solutions, depending on the values of the molecular relaxation rates. Above the instability threshold, a variety of dynamic regimes involving the polarization degree of freedom can be found, including LP states with rotating azimuth (as in incoherently pumped $J=0 \rightarrow J'=1$ or $J=1 \rightarrow J'=0$ lasers), antiphase dynamics, and full polarization chaos.

I. INTRODUCTION

The dynamical behavior of lasers is markedly different in two large classes distinguished by their pumping methods. One method involves incoherent processes (such as, for instance, electrical discharge or light from conventional lamps), whereas the other one is based on a coherent pumping process (typically by means of the light from another laser) in which the pumping and lasing transitions share the common upper level. Two fundamental differences between coherently (optically) and incoherently pumped lasers are known. First, since a laser is generally a source of polarized emission, a polarized pumping beam can break the cylindrical symmetry of the optically pumped laser, even in the case of a perfectly isotropic cavity. Second, coherent pumping induces two-photon (Raman) processes which are absent in an incoherently pumped laser.

The dynamic behavior of these types of lasers has been a subject of extensive investigations [1–3]. However, the problem was typically simplified by the assumption that the laser field had fixed polarization, reducing the vector problem to a scalar one. This simplification was justified by the fact that many lasers were fabricated with Brewster's angle windows or other anisotropic elements which imposed a fixed polarization state.

Recently, the situation has changed. The benefits of the polarization (or vector) degrees of freedom for solving different fundamental and applied problems has renewed the interest in vector systems in general, and in laser systems in particular [4–6]. A large amount of work has already been devoted to different aspects of the static and dynamic behavior of vector laser systems, although most of the work has

been devoted to lasers with incoherent pumping. The influence of the vectorial degrees of freedom on the behavior of lasers with coherent pumping has been less well studied [7–11], although it is evident that polarization freedom should greatly affect their behavior.

Until recently, theoretical studies of vectorial coherently pumped lasers have been restricted to the simplest case which permits full vectorial behavior. In particular, this is the case in which the gain medium is modeled by three-level $J''=0 \rightarrow J=1 \rightarrow J'=0$ atoms with the pumping acting on the $J''=0 \rightarrow J=1$ transition which is adjacent to the laser ($J=1 \rightarrow J'=0$) transition. The Zeeman structure of the upper manifold ($J=1$) enables one to take into account the vectorial degrees of freedom for both pumping and emitted fields. Strong gain anisotropy that favors emission with polarization identical to that of the pump field [7], polarization switching [8], and even full polarization chaos [9,10] have been found in such a system.

However, one may wonder whether the interesting polarization phenomena encountered in the coherently pumped laser are specific to the particular atomic configuration considered, i.e., the $J''=0 \rightarrow J=1 \rightarrow J'=0$ level scheme, or are more general, i.e., weakly sensitive on the particular values of the atomic level quantum numbers J, J', J''. This is an interesting question that arises naturally in the case of, for instance, optically pumped far-infrared molecular lasers. Most of these lasers are coherently pumped by means of a CO_2 or N_2O laser [with wavelengths ranging in the midinfrared ($\lambda \sim 10$ μm)] and their emission wavelength lies in the range $50-500$ μm [12]. With, for instance, the NH_3 laser (one of the most efficient far-infrared lasers), landmark contributions to nonlinear dynamics have been achieved in the past, in particular the first experimental demonstration, in science, of the dynamics of the paradigmatic Lorenz model [13]. The dynamics of this laser, however, are strongly sensitive to the quantum numbers of the molecular levels involved in the pumping-lasing process [for instance, Lorenz-

*Permanent address: Institute of Molecular and Atomic Physics, National Academy of Sciences, F. Skarina Ave., 70, 220072 Minsk, Belarus.

type behavior has only been found in the 81 μm (^{14}NH$_3$) and 153 μm (^{15}NH$_3$) laser emissions but not in the 374 μm (^{15}NH$_3$) emission [2,13–15]]. At this moment it is not known yet whether these differences in behavior are a direct consequence of the differences in the angular momentum quantum numbers of the molecular levels involved, or if they are due to other possible causes such as differences in the molecular relaxation rates [15].

A direct analysis of the specific molecular configurations involved in all these experiments of Refs. [13,14] would be very difficult, because the corresponding angular momentum quantum numbers are high (≥ 2). However, we think that a significant insight into the influence of the angular momentum quantum numbers on the laser dynamics can be gained by investigating molecular configurations with smaller angular momentum quantum numbers. In this paper, we investigate in detail the configuration $J''=1 \rightarrow J=0 \rightarrow J'=1$, where a linearly polarized (LP) pump field acts on the first transition ($J''=1 \rightarrow J=0$) and the laser field acts on the second transition ($J=0 \rightarrow J'=1$) of the Λ-type atomic scheme. Comparison of the results that will be presented here with those obtained in recent years on the $J''=0 \rightarrow J=1 \rightarrow J'=0$ configuration [8–10], as well as with those obtained for an incoherently pumped $J=1 \rightarrow J'=0$ laser [16], will shed light on the problem of the possible dependence of the dynamic behavior on the angular momentum quantum numbers.

The configuration $J''=1 \rightarrow J=0 \rightarrow J'=1$ here studied (as well as other low-J three-level configurations) could in fact be directly implemented in coherently pumped far-infrared lasers by technically modifying the pumping IR laser in order to enlarge its tunability domain. On the other hand, it could also be implemented in an atomic amplification medium such as, for instance, Ne atoms with their three-level configurations $1s_4(J''=1) \rightarrow 2p_3(J=0) \rightarrow 1s_2(J'=1)$ [11] or $2p_7(J''=1) \rightarrow 2s_3(J=0) \rightarrow 2p_2(J'=1)$. In this case, however, Doppler broadening should be taken into account unless an atomic beam is used.

As will be shown below, in spite of the apparently small differences between the configuration $J''=1 \rightarrow J=0 \rightarrow J'=1$ here investigated and the already known $J''=0 \rightarrow J=1 \rightarrow J'=0$ configuration, dramatic changes in the dynamic behavior are found. It is demonstrated, for instance, that the strong gain anisotropy typical of the $J''=0 \rightarrow J=1 \rightarrow J'=0$ configuration disappears and the linearly polarized (LP) modes of the laser with a perfectly isotropic cavity become degenerate in the transverse plane, i.e., with respect to the polarization direction. In other words, axial symmetry in this system is preserved in spite of the presence of a strong and polarized pumping field. On the other hand, we also find emission of circularly polarized (CP) fields, just as in conventional incoherently pumped $J=1 \rightarrow J'=0$ [16] or $J=0 \rightarrow J'=1$ two-level lasers, in spite of the differences between these systems. In particular, four Raman coherences, two one-photon coherences induced by the pumping field, and relaxation processes in the pump-level ($J''=1$) manifold distinguish this laser from an incoherently pumped $J=0 \rightarrow J'=1$ laser (see Fig. 1). These differences mean that above the
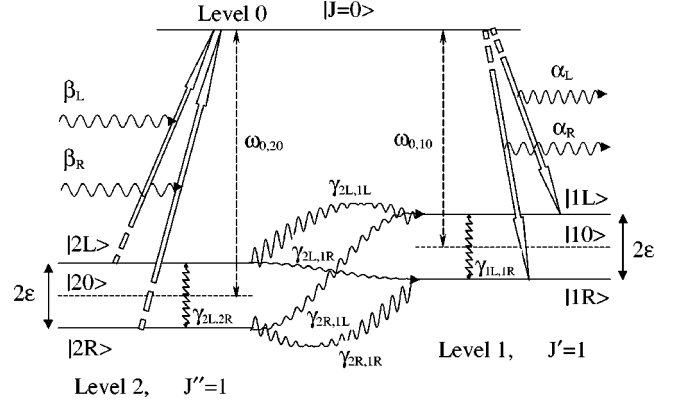

FIG. 1. Level scheme and field components for the coherently pumped laser in ''circular'' basis for atomic states and fields. The sublevels $|2L\rangle$ and $|2R\rangle$ as well as the sublevels $|1L\rangle$ and $|1R\rangle$ are degenerate if no magnetic field ($\varepsilon=0$) is applied. 2β and 2α are the Rabi frequencies for the pump and laser fields, respectively. $\gamma_{2L,1L}$, $\gamma_{2L,1R}$, $\gamma_{2R,1L}$, and $\gamma_{2R,1R}$ are relaxation rates for two photon coherences coupling sublevels of distinct manifolds, whereas $\gamma_{2L,2R}$ and $\gamma_{1L,1R}$ are for the sublevel coherences inside each manifold. The fields propagate in the z direction.

instability threshold both systems display different dynamic polarization states.

We also find that the coherently pumped laser here considered can exhibit some features of a scalar three-level optically pumped laser [17,18], which show up at large pumping strengths when the ac Stark splitting of the upper laser level dominates and leaves the laser field out of resonance. One consequence of this is that with increasing pumping strength, laser emission eventually disappears, either through a pitchfork or an inverse Hopf bifurcation.

The remainder of this paper is the following. In Sec. II, the model for an optically pumped $J''=1 \rightarrow J=0 \rightarrow J'=1$ laser is presented and its general features are discussed. Section III A is devoted to the study of the off state and its stability in the simplified laser model for a perfectly isotropic laser cavity with the laser medium pumped by a LP field. The influence of the material properties on the behavior of the laser steady states is investigated in Sec. III B. Section IV is devoted to numerical stability analysis of the lasing modes. Finally, in Sec. V the main conclusions are summarized.

II. LASER MODEL

In an optically pumped $J''=1 \rightarrow J=0 \rightarrow J'=1$ homogeneously broadened atomic (or molecular) system, a pumping beam drives the first transition and a laser beam is generated on the second transition. The scheme of the atomic levels under consideration is depicted in Fig. 1. The pump level is denoted as 2 and the upper and lower laser levels are denoted as 0 and 1, respectively. The pumping and emitted fields are taken as superpositions of right and left CP fields which are coupled with the corresponding atomic sublevels (Fig. 1).

The states on the $J''=1$ and $J'=1$ manifolds are expressed as linear combinations of $M=+1, 0$, and -1 states. For the $J'=1$ manifold, they will be denoted as $|1L\rangle$, $|10\rangle$,

and $|1R\rangle$, respectively. Similar notations are used to denote the states on the $J''=1$ manifold, i.e., $t|2L\rangle$, $|20\rangle$, and $|2R\rangle$. These six states, plus the $|J=0\rangle$ state, form the atomic basis. In the semiclassical theory adopted here, the states $|20\rangle$ and $|10\rangle$ are not radiatively coupled with any other state by the interaction Hamiltonian (if the pump and laser fields are assumed to propagate in the z direction) and are only coupled through the collisional relaxation process and spontaneous emission, therefore the density matrix has the following relevant elements: seven sublevel populations, which will be denoted as ρ_{kL}, ρ_{k0}, ρ_{kR} $(k=1,2)$, and ρ_0, four induced dipole moments (or one-photon coherences) $\rho_{1L,0}$, $\rho_{1R,0}$, $\rho_{2L,0}$, and $\rho_{2R,0}$, two intersublevel coherences $\rho_{1L,1R}$ and $\rho_{2L,2R}$, and four Raman coherences $\rho_{1R,2L}$, $\rho_{1R,2R}$, $\rho_{1L,2L}$, and $\rho_{1L,2R}$. The decay rates for the one-photon coherences $\rho_{i,0}$ will be denoted as γ_i, with $i=1L$, $1R$, $2L$, and $2R$, and the decay rates for the Raman coherences $\rho_{i,j}$ will be denoted as $\gamma_{i,j}$, with $i,j=1L$, $1R$, $2L$, and $2R$. To take correctly into account the relaxation mechanisms of the level populations and the intersublevel coherences [19,16], it is assumed that the decay rates for the different moments of the triplets 2 and 1 can be different. Specifically, we adopt decay rates γ_{kb}, $\gamma_{kJ}\equiv\gamma_{kb}+\gamma'_{kJ}$, and $\gamma_{kC}\equiv\gamma_{kb}+\gamma'_{kC}$ for the following quantities associated with the $J'=1$ $(k=1)$ and $J''=1$ $(k=2)$ manifolds: total populations $\rho_{kL}+\rho_{k0}+\rho_{kR}$, magnetic dipole $\rho_{kL}-\rho_{kR}$, and "atomic electric quadrupole" $\rho_{kL}+\rho_{kR}-2\rho_{k0}$ as well as intersublevel coherence $\rho_{kL,kR}$, respectively. Incoherent pumping of sublevels $|kL\rangle$, $|kR\rangle$, and $|0\rangle$, which, in the absence of pumping and emitted laser fields, brings the level populations into a stationary thermal-equilibrium state, is taken into account through the corresponding rates λ_{kL}, λ_{kR}, λ_{k0}, and λ_0.

We define the pump and laser field components, in the usual plane-wave uniform-field limit, as

$$\mathbf{E}_{2L(R)}(z,t)=\hat{e}_{L(R)}\frac{\hbar}{\mu_{2L(R)}}\beta_{L(R)}\exp\{i[-k_2z+\omega_2t$$
$$+\varphi_{2L(R)}(t)]\}+\text{c.c.},$$

$$\mathbf{E}_{1L(R)}(z,t)=\hat{e}_{L(R)}\frac{\hbar}{\mu_{1L(R)}}\alpha_{L(R)}(t)\exp\{i[-k_1z+\omega_1t$$
$$+\phi_{1L(R)}(t)]\}+\text{c.c.},\tag{1}$$

respectively, where $\hat{e}_L=(\hat{e}_x-i\hat{e}_y)\sqrt{2}$ and $\hat{e}_R=-(\hat{e}_x+i\hat{e}_y)\sqrt{2}$ are the corresponding unit polarization vectors, $\mu_{2L(R)}$ and $\mu_{1L(R)}$ are the electric-dipole matrix elements which can be taken real, $\beta_{L(R)}$ and $\alpha_{L(R)}(t)$ are one-half of the (real) Rabi frequencies, k_2 (k_1) is the pump (laser) field wave number, and ω_2 and ω_1 are the reference frequencies for the pump and laser fields, respectively. In the following we consider that the pump field is LP, i.e., $\beta_L=\beta_R$, and that its amplitude within the laser cavity is constant and uniform. Thus we neglect pump depletion, which is moderate in gas lasers. $\varphi_{2L(R)}(t)\equiv\theta_{L(R)}+\phi_{2L(R)}$, $\theta_L=\theta_0+\theta(t)$, and $\theta_R=-\theta_0-\theta(t)$, where the parameter θ_0 is the relative orientational angle between the polarization plane of the pumping field and the reference direction, the parameter $\theta(t)$ would de-

scribe the variation of the azimuth angle of the pumping field vector in the case of pump polarization modulation, and $\phi_{2L(R)}$ and $\phi_{1L(R)}(t)$ are the phases of the pump and laser fields in the absence of any modulation of the pumping field, respectively, so that $\omega_2+\dot{\varphi}_{2L(R)}(t)$ and $\omega_1+\dot{\phi}_{1L(R)}(t)$ represent the instantaneous pump and laser field frequencies. c.c. denotes complex conjugate. Thus note that both the amplitude $\alpha_{L(R)}(t)$ and phase of the generated laser field can be time-dependent, in a dynamic regime.

It is convenient to extract explicitly the frequencies ω_k and phases $\phi_{kL(R)}$ of the laser and pumping fields from all complex elements of the density matrix, leaving the same notations for the new density-matrix elements. After that, the Maxwell-Bloch equations for the laser can be written, in the usual rotating-wave and slowly varying envelope approximations, in the circular basis, and in their most general form which allows for the possible presence of cavity anisotropies and a longitudinal magnetic field, as

$$\dot{\rho}_0=2\alpha_L\,\text{Im}\,\rho_{1L,0}+2\alpha_R\,\text{Im}\,\rho_{1R,0}$$
$$+2\beta_L(\text{Im}\,\rho_{2L,0}\cos\theta_L-\text{Re}\,\rho_{2L,0}\sin\theta_L)$$
$$+2\beta_R(\text{Im}\,\rho_{2R,0}\cos\theta_R-\text{Re}\,\rho_{2R,0}\sin\theta_R)-\gamma_0\rho_0+\lambda_0,$$

$$\dot{\rho}_{1L}=-\Gamma_{1P}\rho_{1L}-\Gamma_{1M}\rho_{1R}+\gamma'_{1C}\rho_{10}/3-2\alpha_L\,\text{Im}\,\rho_{1L,0}+\lambda_{1L},$$

$$\dot{\rho}_{1R}=-\Gamma_{1P}\rho_{1R}-\Gamma_{1M}\rho_{1L}+\gamma'_{1C}\rho_{10}/3-2\alpha_R\,\text{Im}\,\rho_{1R,0}+\lambda_{1R},$$

$$\dot{\rho}_{10}=-(\gamma_{1b}+2\gamma'_{1C}/3)\rho_{10}+\gamma'_{1C}(\rho_{1L}+\rho_{1R})/3+\lambda_{10},$$

$$\dot{\rho}_{2L}=-\Gamma_{2P}\rho_{2L}-\Gamma_{2M}\rho_{2R}+\gamma'_{2C}\rho_{20}/3-2\beta_L(\text{Im}\,\rho_{2L,0}\cos\theta_L$$
$$-\text{Re}\,\rho_{2L,0}\sin\theta_L)+\lambda_{2L},$$

$$\dot{\rho}_{2R}=-\Gamma_{2P}\rho_{2R}-\Gamma_{2M}\rho_{2L}+\gamma'_{2C}\rho_{20}/3-2\beta_R(\text{Im}\,\rho_{2R,0}\cos\theta_R$$
$$-\text{Re}\,\rho_{2R,0}\sin\theta_R)+\lambda_{2R},$$

$$\dot{\rho}_{20}=-(\gamma_{2b}+2\gamma'_{2C}/3)\rho_{20}+\gamma'_{2C}(\rho_{2L}+\rho_{2R})/3+\lambda_{20},$$

$$\dot{\rho}_{1L,0}=-i(\Delta_{1L}(t)+\varepsilon+\gamma_{1L})\rho_{1L,0}-i[\alpha_Ld_{0,1L}-\alpha_R\rho_{1L,1R}$$
$$-\beta_L\rho_{1L,2L}\exp(i\theta_L)-\beta_R\rho_{1L,2R}\exp(i\theta_R)],$$

$$\dot{\rho}_{1R,0}=-i(\Delta_{1R}(t)-\varepsilon+\gamma_{1R})\rho_{1R,0}-i[\alpha_Rd_{0,1R}-\alpha_L\rho_{1R,1L}$$
$$-\beta_L\rho_{1R,2L}\exp(i\theta_L)-\beta_R\rho_{1R,2R}\exp(i\theta_R)],$$

$$\dot{\rho}_{2L,0}=-i(\Delta_{2L}+\varepsilon+\gamma_{2L})\rho_{2L,0}-i[\beta_Ld_{0,2L}\exp(i\theta_L)$$
$$-\alpha_L\rho_{2L,1L}-\alpha_R\rho_{2L,1R}-\beta_R\rho_{2L,2R}\exp(i\theta_R)],$$

$$\dot{\rho}_{2R,0}=-i(\Delta_{2R}-\varepsilon+\gamma_{2R})\rho_{2R,0}-i[\beta_Rd_{0,2R}\exp(i\theta_R)$$
$$-\alpha_L\rho_{2R,1L}-\alpha_R\rho_{2R,1R}-\beta_L\rho_{2R,2L}\exp(i\theta_L)],$$

$$\dot{\rho}_{1L,1R}=-i[\Delta_{1L}(t)-\Delta_{1R}(t)+2\varepsilon]\rho_{1L,1R}-i(\alpha_L\rho_{0,1R}$$
$$-\alpha_R\rho_{1L,0})-\gamma_{1C}\rho_{1L,1R},$$

$$\dot{\rho}_{2L,2R} = -i(\Delta_{2L} - \Delta_{2R} + 2\varepsilon)\rho_{2L,2R} - i[\beta_L \rho_{0,2R} \exp(i\theta_L)$$

$$- \beta_R \rho_{2L,0} \exp(-i\theta_R)] - \gamma_{2C}\rho_{2L,2R},$$

$$\dot{\rho}_{1R,2L} = -i[\Delta_{1R}(t) - \Delta_{2L} - 2\varepsilon]\rho_{1R,2L} - i[\alpha_R \rho_{0,2L}$$

$$- \beta_L \rho_{1R,0} \exp(-i\theta_L)] - \gamma_{1R,2L}\rho_{1R,2L},$$

$$\dot{\rho}_{1R,2R} = -i[\Delta_{1R}(t) - \Delta_{2R}]\rho_{1R,2R} - i[\alpha_R \rho_{0,2R}$$

$$- \beta_R \rho_{1R,0} \exp(-i\theta_R)] - \gamma_{1R,2R}\rho_{1R,2R},$$

$$\dot{\rho}_{1L,2L} = -i[\Delta_{1L}(t) - \Delta_{2L}]\rho_{1L,2L} - i[\alpha_L \rho_{0,2L} - \beta_L \rho_{1L,0}$$

$$\times \exp(-i\theta_L)] - \gamma_{1L,2L}\rho_{1L,2L},$$

$$\dot{\rho}_{1L,2R} = -i[\Delta_{1L}(t) - \Delta_{2R} + 2\varepsilon]\rho_{1L,2R} - i[\alpha_L \rho_{0,2R} - \beta_R \rho_{1L,0}$$

$$\times \exp(-i\theta_R)] - \gamma_{1L,2R}\rho_{1L,2R}, \tag{2}$$

$$\dot{\alpha}_L = -\kappa\alpha_L - g_L \operatorname{Im} \rho_{1L,0} + \kappa'_L \alpha_L + \alpha_R(\zeta'_R \cos 2\Phi$$

$$+ \zeta''_R \sin 2\Phi),$$

$$\dot{\alpha}_R = -\kappa\alpha_R - g_R \operatorname{Im} \rho_{1R,0} + \kappa'_R \alpha_R + \alpha_L(\zeta'_L \cos 2\Phi$$

$$+ \zeta''_L \sin 2\Phi),$$

$$\dot{\phi}_{1L} = (\Delta_{1L} - \Delta_c + \kappa''_L) + g_L \operatorname{Re} \rho_{1L,0}/\alpha_L + \alpha_R(\zeta''_R \cos 2\Phi$$

$$- \zeta'_R \sin 2\Phi)/\alpha_L,$$

$$\dot{\phi}_{1R} = (\Delta_{1R} - \Delta_c + \kappa''_R) + g_R \operatorname{Re} \rho_{1R,0}/\alpha_R + \alpha_L(\zeta''_L \cos 2\Phi$$

$$+ \zeta'_L \sin 2\Phi)/\alpha_R,$$

where $\Gamma_{iP} = \gamma_{ib} + \gamma'_{iC}/6 + \gamma'_{iJ}/2$ and $\Gamma_{iM} = \gamma'_{iC}/6 - \gamma'_{iJ}/2$ ($i = 1,2$); $d_{0,kL} = (\rho_0 - \rho_{kL})$ and $d_{0,kR} = \rho_0 - \rho_{kR}$; $\Delta_{1L(R)}(t) = \Delta_1 + \dot{\phi}_{1L(R)}(t)$; $\Delta_k = \omega_k - \omega_{0,k0}$ are the detunings of the pump ($k=2$) and laser ($k=1$) fields with respect to the atomic resonances; $\omega_{0,10}$ and $\omega_{0,20}$ are the frequency separations between the level $J=0$ and the lower sublevels $J' = 1, M = 0$ and $J'' = 1, M = 0$, respectively (Fig. 1); $\Delta_c = \omega_c - \omega_{0,10}$ is the cavity detuning (ω_c is the empty-cavity resonance frequency); $g_{L(R)}$ is the unsaturated gain parameter and the parameter κ is the cavity decay rate. Cavity anisotropies are additively taken into account in the field equations through complex direct $\kappa_{L(R)} \equiv \kappa'_{L(R)} + i\kappa''_{L(R)}$ and cross $\zeta_{L(R)} \equiv \zeta'_{L(R)} + i\zeta''_{L(R)}$ losses of the left (right) CP harmonic of the laser field, with $\Phi \equiv (\phi_{1L} - \phi_{1R})/2$ being the polarization azimuth of the emitted field. The parameter $\varepsilon = \mu_B G_L |\mathbf{B}|/\hbar$ (where μ_B is the Bohr magneton and G_L the Landé factor, assumed for simplicity to be equal for both lower levels) describes the modulus of the shift of the levels $|kL\rangle$ and $|kR\rangle$ that would appear upon introduction of a longitudinal magnetic field $\mathbf{B}$ (Fig. 1). When only linear amplitude and phase anisotropies are present, direct and cross losses can be written in the form $\kappa_L = \kappa_R = c/2nL\{(p_x + p_y)\cos\Delta - 2 + i(p_x - p_y)\sin\Delta\}c/2nL$ and $\zeta_L = \zeta_R = c/2nL\{(p_x - p_y)\cos\Delta + i(p_x + p_y)\sin\Delta\}c/2nL$, where nL/c is the cavity round-trip time (c

is the speed of light in vacuum, nL is the optical length of the cavity). Parameters $p_{x,y}$ are the amplitude transmissions of the cavity for the laser field polarized in the x and y directions; i.e., they are quantities within the range $[0,1]$. Their maximum values, i.e., $p_x = p_y = 1$, correspond to the absence of anisotropic absorption in the cavity (obviously, the cavity can have *isotropic* losses κ). Any anisotropy (in the x and y directions) reduces these quantities leading to negative values for parameters κ'_L and κ'_R. Parameter Δ is the cavity linear phase anisotropy which is measured in radians (for example, there is no phase anisotropy when $\Delta = 0$, whereas $\Delta = \pi/4$ corresponds to a quarter wave plate).

Since the present model can be applied to far-infrared lasers, which are class-C lasers [1,2,20], we cannot introduce drastic simplifications in the laser equations such as, for instance, adiabatic elimination of the one-photon or Raman coherences or the population inversion (other less fundamental simplifications, however, will be introduced below). On the other hand, our model in principle only applies to molecular or atomic configurations. It would hardly apply to a solid-state laser medium, where the energy levels of the active ions are often broadened by coupling with phonons and by the crystal field and they can be affected by orbital angular momentum quenching, or to a semiconductor laser medium, where the electronic states form bands rather than discrete states, the dispersive effects are described by the so-called α factor [21], and the dipole relaxation rate is very large (it might apply to a quantum-well laser system, but there the dominating angular momenta take other values, and these lasers still keep to a certain degree the specific features of semiconductor materials).

Several important features can be extracted from the full set of laser equations (2). First, the global laser-field phase $\Phi_s \equiv \phi_{1L} + \phi_{1R}$ does not appear in the equations, as occurs in general in autonomous laser systems (note, however, that our laser system becomes nonautonomous when the pump field polarization vector is modulated, since the parameters θ_L and θ_R become time-dependent). Second, in the absence of cavity anisotropies the laser equations (2) are insensitive to the phase difference between the CP harmonics of the laser field. In other words, neither the material dynamics nor the polarized pumping field fix the polarization azimuth of the total laser field. This results in sharp contrast with what is found in the case of an optically pumped $J'' = 0 \rightarrow J = 1 \rightarrow J' = 0$ laser studied in Refs. [7–10], where the polarization state of the emitted field is always uniquely determined. However, the present result is similar to what was found in the case of an incoherently pumped $J = 1 \rightarrow J' = 0$ laser [16] in which the polarization azimuth is free to diffuse if the laser cavity is perfectly isotropic (only cavity anisotropies could break the axial symmetry and fix the polarization azimuth). This preliminary analysis suggests that the behavior of our laser system will have features similar to that found in the incoherently pumped laser.

III. SOLUTIONS

We study next the steady-state solutions of the laser system and their stability. To make the problem as tractable

analytically as possible, several approximations will be adopted. We will concentrate on a laser operating at resonance $[\Delta_c = \Delta_{1L} = \Delta_{1R} = 0$; we have checked numerically that in general $\Delta_c = 0$ implies $\Delta_{1L}(t) = \Delta_{1R}(t) = 0$, except for certain time-dependent solutions that are described in Sec. IV], with no external perturbations such as a magnetic field ($\varepsilon = 0$) or a pump-field polarization modulation $[\theta(t) = 0]$. It will be assumed that the pumping field is LP along the x direction, i.e., $\beta_L = \beta_R \equiv \beta$ and $\theta_0 = 0$ (although, for checking the dependence of the laser emission on the pump polarization angle, θ_0 will be retained as a control parameter in some numerical simulations). The decay rates of the one-photon coherences induced by the laser field will be taken to be identical and denoted as $\gamma_\perp \equiv \gamma_{1L} = \gamma_{1R}$. It is also physically reasonable to assume that $\gamma_{2L} = \gamma_{2R} \equiv \gamma_\beta$; $\gamma_{1R,2L} = \gamma_{1L,2L} \equiv \gamma_{LPh}$; $\gamma_{1R,2R} = \gamma_{1L,2R} \equiv \gamma_{RPh}$. All control parameters will be rescaled with respect to the transverse decay rate $\gamma_\perp$. This means, in particular, that, since we are considering the most general case of a class-C laser, all molecular and field relaxation rates will be $O(1)$—in the specific case of a far-infrared molecular laser the absolute value of these relaxation rates is of the order of 10^6 s^{-1} [1,12]. Accordingly, time will be expressed in units of $\gamma_\perp^{-1}$. We will also assume that the laser cavity and gain are isotropic, i.e., $\kappa'_{L(R)} = \kappa''_{L(R)} = \zeta'_{L(R)} = \zeta''_{L(R)} = 0$ and $g_L = g_R = g$. And, finally, incoherent pumping rates of the sublevels $|kL\rangle$ and $|kR\rangle$ ($k = 1,2$) in the two $J = 1$ manifolds will be taken identical, i.e., $\lambda_{kL} = \lambda_{kR} \equiv \lambda_k$, while $\lambda_{10} = \lambda_{20} = 0$.

A. The off solution and its stability

Under these assumptions, the laser equations (2) yield an off solution with zero intensities ($\alpha_L^2 = \alpha_R^2 = 0$) of the CP components of a single mode laser field, and

$$\text{Im}\,\rho_{2L,0} = \text{Im}\,\rho_{2R,0} = \gamma_{2C}\beta B_0, \quad \text{Re}\,\rho_{2L,2R} = -2\beta^2 B_0,$$

$$\rho_0 = (4\beta^2 \gamma_{2C} B_0 + \lambda_0)/\gamma_0, \quad \rho_{10} = 2\lambda_1(\gamma_{1C} - \gamma_{1b})/3\gamma_{1b}\gamma_{1C},$$

$$\rho_{1L} = \rho_{1R} = \lambda_1(\gamma_{1b} + 2\gamma_{1C})/3\gamma_{1b}\gamma_{1C},$$

$$\rho_{2L} = \rho_{2R} = (\lambda_2 - 2\beta^2 \gamma_{2C} B_0)(\gamma_{2b} + 2\gamma_{2C})/3\gamma_{2b}\gamma_{2C},$$

$$\rho_{20} = 2(\lambda_2 - 2\beta^2 \gamma_{2C} B_0)(\gamma_{2C} - \gamma_{2b})/3\gamma_{2b}\gamma_{2C},$$

$$\rho_{1L(R),0} = \text{Re}\,\rho_{2L(R),0} = \rho_{1L,1R} = \text{Im}\,\rho_{2L,2R} = \rho_{R,2L} = \rho_{R,2R}$$

$$= \rho_{L,2L} = \rho_{L,2R} = 0,$$

(3)

where the coefficient B_0 is given in the Appendix.

It can be seen that the lower laser level 1 is only populated by the incoherent pumping (and it is zero when $\lambda_1 = 0$). Populations of the other two levels are created by both coherent and incoherent pumping. Expressions for ρ_{10} and ρ_{20} constrain the value of γ_{kC}, which must be greater than or equal to γ_{kb} (note that $\lambda_2 - 2\beta^2 \gamma_{2C} B_0 > 0$).

The stability of this off solution is governed by the set of eigenvalues of the linearized equations for perturbations of the system variables. Our analysis reveals that the full set of

linearized equations (or the corresponding Jacobian matrix) can be separated into several subsets, of which only two can yield positive eigenvalues and are relevant from the physical point of view. These subsets correspond to the variables $\{\text{Im}\,\rho_{1L,0}; \text{Re}\,\rho_{1L,2L}; \text{Re}\,\rho_{1L,2R}; \alpha_L\}$ and $\{\text{Im}\,\rho_{1R,0}; \text{Re}\,\rho_{1R,2L}; \text{Re}\,\rho_{1R,2R}; \alpha_R\}$, respectively. As can be seen, the equations for the left and right CP components of the laser field belong to distinct subsets, which means that the stability conditions of the off solution with respect to the perturbation of each of the components are, in general, different. However, in the limit of no linear (i.e., independent of the laser/pump intensity) anisotropy, these two matrices are identical, which means that in such a limit the off solution will lose its stability at the same parameter values independent of the polarization state of the perturbation.

The fourth-degree characteristic polynomial determining the stability of the off solution (see the Appendix) is independent of γ_J, which is a consequence of the fact that the populations of the sublevels $|kL\rangle$ and $|kR\rangle$ in the two manifolds 1 and 2 are identical ($\rho_{1L} = \rho_{1R}$ and $\rho_{2L} = \rho_{2R}$). According to the Hurwitz criterion, the off solution can be destabilized through either a pitchfork bifurcation (PB) or a Hopf bifurcation (HB)—see the Appendix. The PB occurs at pump intensity values given by

$$\beta_{PB}^2 = \{-A_2 \pm (|A_2| - 24\kappa\gamma_{LPh}\gamma_{RPh}\gamma_{2b}\gamma_{2C}\gamma_\beta\gamma_{SPh}$$
$$\times A_1 A_3 / |A_2|)\}/8\kappa A_1 \gamma_{SPh}, \tag{4}$$

where the coefficients A_1, A_2, and A_3 are given in the Appendix.

Expression (4) shows that the trivial solution can be stable in two domains of pumping strength. One of these domains corresponds to low pumping and extends up to a pump value known as a first laser threshold, β'_{PB}, which is defined by the minus sign in Eq. (4). The second domain is above a large pumping threshold β''_{PB}, which is determined by the plus sign in Eq. (4). Physically, this second domain at large pumping exists because of the large ac Stark shifting of the laser levels induced by the strong pumping field [8,17,18,22] which carries the transition out of resonance.

It is worth pointing out what would occur in the case when in addition to the coherent optical pumping there is also a significant source of incoherent pumping described by the parameter λ_0. In this case, when λ_0 increases the first threshold β'_{PB} decreases, and when $\lambda_0 \geq \gamma_0(\rho_{1L} + \kappa/g)$, the solution to Eq. (4) corresponding to the minus sign becomes unphysical ($\beta_{PB}^2 < 0$), i.e., the PB β'_{PB} disappears and thus the laser will operate for any pumping $\beta < \beta''_{PB}$, in particular for $\beta = 0$, which means that the incoherent pumping itself is sufficient to switch on the laser system.

Unlike the PB, the Hopf bifurcation is determined by a lengthy algebraic expression of the eighth degree with respect to the pumping strength (with only odd powers of β). Consequently, an explicit analytical solution to this equation cannot be obtained and it must be solved numerically. In the next section graphical results showing the dependence of the pitchfork and Hopf bifurcation thresholds on several laser parameters are shown.

B. Lasing steady-state solutions

On resonance (and with no magnetic field, $\varepsilon = 0$, and $\theta_L = \theta_R = 0$) the lasing equations (2) become considerably simpler since all of them will be real. Analysis reveals that in contrast to the case of an optically pumped $J'' = 0 \rightarrow J = 1 \rightarrow J' = 0$ laser, Eq. (2) admit both LP and *circularly polarized* (CP) lasing steady states in spite of the presence of a strong LP pumping field. To obtain tractable exact analytical expressions for the steady states, we will neglect the small incoherent pumping rates λ_0 and λ_1 (i.e., $\lambda_0 = \lambda_1 = 0$), we will reasonably assume that $\gamma_{1b} = \gamma_{2b} \equiv \gamma_b$, $\gamma'_{1J} = \gamma'_{2J} \equiv \gamma'_J$, and $\gamma'_{1C} = \gamma'_{2C} \equiv \gamma'_C$ (i.e., that in both manifolds decay rates of each tensorial component are equal), and we set $\lambda_2 = \gamma_0 = 1$ and $\gamma_\beta = \gamma_{LPh} = \gamma_{RPh} = 1$.

The intensity of the left CP solution reads

$$I_L \equiv \alpha_L^2 = \{\kappa A \pm \sqrt{\kappa^2 A^2 - 36B\,\gamma_b^2\gamma_J\gamma_C^2\kappa(6\,\gamma_b\gamma_J\gamma_C + \gamma_M)}\}/6\kappa\gamma_b\gamma_C(6\,\gamma_b\gamma_J\gamma_C + \gamma_M). \tag{5}$$

For the sake of brevity we do not retain here analytical expressions for the nonzero one- and two-photon coherences $\text{Im}\,\rho_{2L,0} = \text{Im}\,\rho_{2R,0}$, $\text{Re}\,\rho_{1L,2L} = \text{Re}\,\rho_{1L,2R}$, $\text{Im}\,\rho_{1L,0}$, and $\text{Re}\,\rho_{2L,2R}$. The expressions for the populations as well as for the parameters A, B, and γ_M are given in the Appendix.

Because of the square root in Eq. (5), there are in general two left CP solutions, with different intensity. Each of these solutions has a symmetric right CP solution of the same intensity, which can be obtained with the following substitution: $\alpha_L \rightarrow \alpha_R$, $\text{Re}\,\rho_{1L,2L} = \text{Re}\,\rho_{1L,2R} \rightarrow \text{Re}\,\rho_{1R,2L} = \text{Re}\,\rho_{1R,2R}$, $\text{Im}\,\rho_{1L,0} \rightarrow \text{Im}\,\rho_{1R,0}$, and $\rho_{1L} \rightarrow \rho_{1R}$.

For the LP solution the intensities of its two CP harmonics α_L^2 and α_R^2 are equal and read

$$\alpha_L^2 = \alpha_R^2 = (\kappa C \pm \sqrt{\kappa^2 C^2 - 72\kappa\gamma_b^2\gamma_C^2\gamma_P B})/24\kappa\gamma_b\gamma_C\gamma_P, \tag{6}$$

so that the total intensity of the LP solution is $I_{\text{lin}} = \alpha_L^2 + \alpha_R^2$. The populations and the parameter C are given in the Appendix. The other nonzero variables verify $\text{Im}\,\rho_{2L,0} = \text{Im}\,\rho_{2R,0}$, $\text{Re}\,\rho_{1L,2R} = \text{Re}\,\rho_{1R,2R} = \text{Re}\,\rho_{1L,2L} = \text{Re}\,\rho_{1R,2L}$, $\text{Im}\,\rho_{1L,0} = \text{Im}\,\rho_{1R,0}$, $\text{Re}\,\rho_{1L,1R}$, and $\text{Re}\,\rho_{2L,2R}$.

Similar to the previous case, in general, Eq. (6) admits two solutions of different intensity. These solutions do not depend on the decay rate γ_J. This is a direct consequence of the fact that the populations of the sublevels of each $J = 1$ manifold (levels 1 and 2) are equal $\rho_{kL} = \rho_{kR}$ ($k = 1,2$) (see the Appendix), which is not the case for CP states. There is a correspondence between the CP and LP solutions, in the sense that when $\gamma'_J = \gamma'_C$ (for which $A = C\gamma_C$) the intensity of each CP solution coincides with that of a LP solution $I_{L(R)} = I_{\text{lin}}$. Note that in the presence of the left (right) CP mode the sublevel $1R$ ($1L$) is always populated provided that $\gamma'_J > \gamma'_C$. Its population takes on a zero value in the radiative limit ($\gamma'_J = \gamma'_C = 0$).

One important feature of the LP solutions (6) is that, as advanced above, their azimuth can take any value, i.e., it is not determined by the pump-field polarization azimuth nor by the field-matter interaction processes. This is similar to what occurs with the incoherently pumped two-level $J = 1 \rightarrow J' = 0$ laser [16] (in conditions, as here, of isotropic cavity), and is in sharp contrast with the behavior of the optically pumped $J'' = 0 \rightarrow J = 1 \rightarrow J' = 0$ laser, for which the field-matter interaction imposes a strong correlation between the pump- and laser-field polarization states [10].

The mathematical requirement that expressions (5) and (6) must be real and non-negative determines the domains in the parameter space where the steady states exist. These domains are linked to the domain where the off solution is unstable, which has been discussed in the preceding subsection. We discuss next the dependence of these domains on several laser parameters, such as β, γ_b, γ'_J, and γ'_C.

Inspection of these equations shows the following features.

(i) The coefficients A and C are generally negative, which excludes the possibility of the existence of two lasing solutions in any of these equations; i.e., only one LP and one couple of CP solutions with opposite helicity are possible. This is strictly valid for $0 \leqslant \gamma_b \leqslant (1 + \sqrt{2})/3 \approx 0.8$, for any value of all the other laser parameters. For larger γ_b [i.e., for $(1 + \sqrt{2})/3 \leqslant \gamma_b \leqslant 1$, since in our case, for physical reasons, γ_b cannot be above $\gamma_\perp$], the coefficients A and C can become positive whenever γ'_C is above a threshold value $\gamma_{C(\text{circ})} \equiv \gamma_b + \gamma'_{C(\text{circ})}$ (for A) and $\gamma'_{C(\text{lin})}$ (for C) given, respectively, by the conditions

$$(9\gamma_b^2 - 18\gamma_J\gamma_b^2 + 12\gamma_J\gamma_b + 3\gamma_b + 2\gamma_J)\gamma_{C(\text{circ})}^2$$
$$+ \gamma_b(6\gamma_b + 15\gamma_J\gamma_b + 5\gamma_J)\gamma_{C(\text{circ})} + 2\gamma_J\gamma_b^2 = 0, \tag{7}$$
$$\gamma'_{C(\text{lin})} = 3\gamma_b(3\gamma_b^2 - 4\gamma_b - 1 - 2\sqrt{2}\gamma_b)/(1 + 6\gamma_b - 9\gamma_b^2).$$

The curves representing $\gamma'_{C(\text{circ})}$ and $\gamma'_{C(\text{lin})}$ as a function of γ_b are depicted in Fig. 2. Clearly, the large values necessary for γ'_C indicate that in realistic conditions A and C will be negative.

(ii) When the pump amplitude β is continuously increased from zero, the coefficient B (which includes the pump intensity β^2 and the cavity losses κ, among other parameters) in Eqs. (5) and (6) starts with a positive value (laser off state) and continuously decreases. When it crosses zero, changing from a positive to a negative value, a single LP solution [the case of Eq. (6)] or a single couple of CP solutions with opposite helicity [the case of Eq. (5)] appears, thus defining the first laser threshold. The value of β at
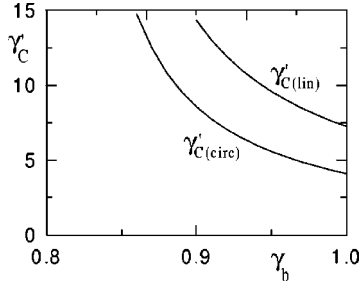
FIG. 2. Values of $\gamma'_{C(\text{lin})}$ and $\gamma'_{C(\text{circ})}$ below which the system shows only one LP or CP solution, as a function of the population relaxation rate γ_b.

which this occurs coincides with the value of β'_{PB} corresponding to the first PB point of the off solution discussed in the preceding section.

(iii) Above the first laser threshold, where $B < 0$, the modulus of B first increases and next decreases, crossing again zero. This means that the laser intensity first increases and next decreases, disappearing at a large pump amplitude value β which coincides with the second PB β''_{PB} of the off solution already discussed in Sec. III A. Both points β'_{PB} and β''_{PB} are the same for the LP and CP solutions, as pointed out above.

These features (ii) and (iii) can be seen in Fig. 3, which shows the emission intensity of the CP and LP solutions as a function of the pump-field amplitude β. The two PB points β'_{PB} and β''_{PB} can be clearly identified, and it is seen that since $\gamma_C > \gamma_J$ the intensity of the LP solution is slightly larger than that of the CP solution (the contrary would occur for $\gamma_C < \gamma_J$).

IV. STABILITY OF THE LASING STEADY STATES

Since the first laser threshold β_{PB} is common for both LP and CP solutions, what occurs just above threshold is determined by the so-called maximum emission principle: only the branch with larger emission intensity, which for γ_C
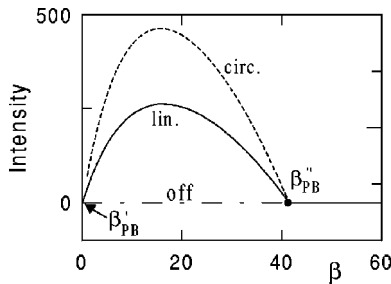

FIG. 3. Off solution (off), full intensity (I_L) of the CP solution (circ), and half of the intensity ($I_{\text{lin}}/2$) of the LP solution (lin) (it is depicted just for the sake of clarity; full intensities of both solutions would be barely distinguishable) plotted versus pumping strength β for $\gamma_b = 0.3$, $\gamma'_C = 0.5$, $\gamma'_J = 0.2$. Full curves show stable branches (we note that the total intensity of the stable LP solution is slightly larger than that of the CP one) of LP and off solutions. Dashed line represents unstable solutions. Dashed-dotted line shows unstable branch of the off solution.
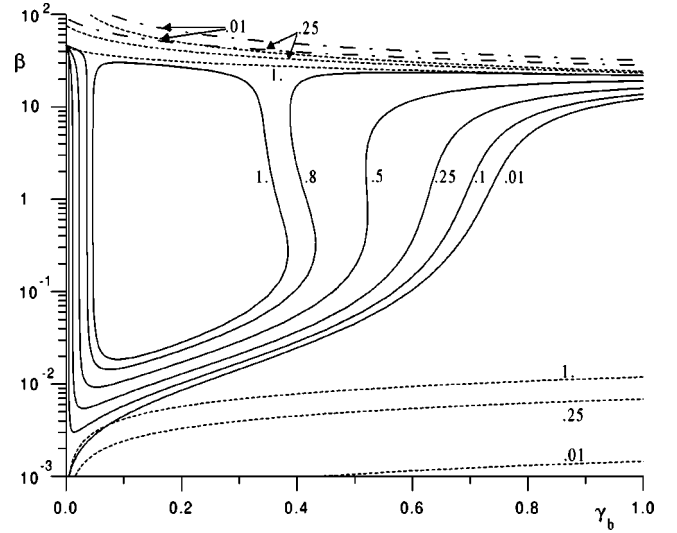

FIG. 4. The on (β'_{PB}, lower dashed lines) and off (β''_{PB}, upper dashed lines) thresholds of the static CP mode and the Hopf bifurcations of the trivial (dashed-dotted lines) and lasing (continuous lines) states are shown in the subspace (β, γ_b) for different decay rates of the upper-level population (given in the figure). Other parameters are fixed at $\lambda_{2L} = \lambda_{2R} = 0.5$, $\gamma_\beta = \gamma_{Ph} = 1$, $g = 3642.5$, $\kappa = 1.425$, $\gamma'_J = 0.5$, $\gamma'_C = 0.3$, and the remaining parameters are the same as those adopted in Sec. II. Lasing solution is stable ''below'' the corresponding continuous curves. It exists in between the dashed lines.

$> \gamma_J$ ($\gamma_C < \gamma_J$) is the linearly (circularly) polarized one, is stable. This is different from what occurs in the case of the coherently pumped $J'' = 0 \rightarrow J = 1 \rightarrow J' = 0$ laser, where this factor (i.e., the maximum emission intensity) is rapidly counterbalanced by a strong pump-induced anisotropy which favors a polarization state identical to that of the pump beam.

Let us assume that $\gamma_C < \gamma_J$ and analyze numerically the stability of the CP steady-state solution along all the domain above the first laser threshold (qualitatively similar results would be found in the opposite case $\gamma_C > \gamma_J$ concerning the stability of the LP solution). We will fix some parameters: $\Delta_c = 0$, $\lambda_{2L} = \lambda_{2R} = 0.5$, $g = 3642.5$, and $\kappa = 1.425$. This choice of the cavity losses κ ensures that for small and moderate atomic decay rates the laser system will be in the ''bad cavity limit'' [i.e., the condition $\kappa > \gamma_\parallel + \gamma_\perp$ will be fulfilled; here $\gamma_\parallel^{-1} = (\gamma_0^{-1} + \gamma_b^{-1})/2$]. Later on, other values of κ will also be considered. For the rest of the parameters, we will suppose fewer restrictions than in Sec. III B, namely, $\Delta_c = \Delta_{1L} = \Delta_{1R} = \Delta_{2L} = \Delta_{2R} = 0$, $\gamma'_{1J} = \gamma'_{2J} \equiv \gamma'_J$, $\gamma'_{1C} = \gamma'_{2C} \equiv \gamma'_C$, $\gamma'_{2L} = \gamma'_{2R} \equiv \gamma_\beta$, $\gamma_{1b} = \gamma_{2b} \equiv \gamma_b$, $\gamma_\perp = 1$, and $\gamma_{RPh} = \gamma_{LPh} \equiv \gamma_{Ph}$. We will also allow for the possibility that the instantaneous laser-field frequency might be different from the resonance frequency [i.e., $\Delta_{1L}(t)$ or $\Delta_{1R}(t)$ are different from 0].

Figure 4 shows the pump amplitude values at which different local bifurcations affect the off and CP steady-state solutions, as a function of the lower-level population relaxation rate γ_b and for different values of the upper-level population relaxation rate γ_0. The dashed lines correspond to the β'_{PB} and β''_{PB} bifurcation thresholds affecting the off solution
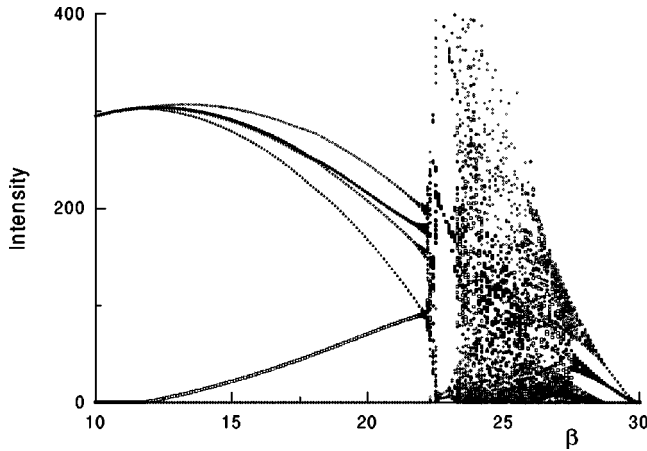
FIG. 5. One-parameter diagram of the field intensities vs pump magnitude β for $\gamma_0 = 0.5$, $\gamma_b = 0.6$. Open points (crosses), dots (triangles), and squares (rhombuses) show maxima (minima) of the total intensity, levo, and dextro CP components, respectively. Other parameters correspond to Fig. 4.
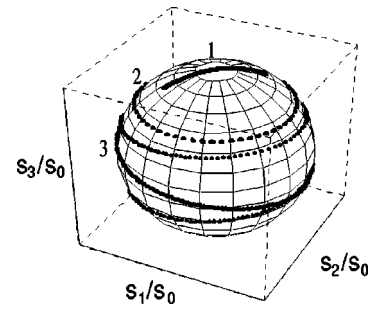

FIG. 6. Trajectory of the laser field polarization state on the Poincaré sphere in the cases of Fig. 5 (1), Fig. 7(b) (2), and Fig. 7(a) (3) for $\beta = 15$. s_0, s_1, s_2, and s_3 are the Stokes parameters, as defined for instance in E. Hecht and A. Zajac, *Optics* (Addison-Wesley, Reading, 1974).

as described in Sec. III A. Thus, the steady-state solution exists in the wide domain of pump amplitudes delimited by these two curves. The dashed-dotted line corresponds to the Hopf bifurcation that also affects the off solution at very large pump amplitudes (see also Sec. III A). The continuous line describes the threshold for another Hopf bifurcation β_{HB}, which affects the lasing steady-state solution. As can be seen in the figure, in general this bifurcation is unique except for small values of γ_b and large values of γ_0, where a second HB can appear at large pump amplitudes. A HB also appears in related laser systems such as the three-level (scalar) optically pumped laser, the optically pumped $J'' = 0 \rightarrow J = 1 \rightarrow J' = 0$ laser, and the incoherently pumped $J = 0 \rightarrow J' = 1$ laser, but its origin and pump threshold as well as the dynamic behavior above the bifurcation threshold are very different in each case. The largest qualitative similarity is with the incoherently pumped $J = 0 \rightarrow J' = 1$ laser, where above the HB threshold the modulated state that appears loses very fast its stability and the system falls in general onto a state with linear polarization with rotating azimuth ("rotating linear" behavior) [16]. In our case, however, the behavior is not exactly the same and depends on the operating conditions, as we show next with some illustrative examples.

Figure 5 shows the emission intensity as a function of β for conditions corresponding to the right-hand part of Fig. 4, i.e., for large γ_b ($\gamma_b = 0.6$ in this case but a similar behavior is found above this value) and any value of γ_0 ($\gamma_0 = 0.5$ in this case). As indicated in Fig. 4, for this case the laser emission threshold is at $\beta_{PB} \approx 0.65 \times 10^{-2}$ and the HB affecting the steady-state solution (which in the example of Fig. 5 is a levo CP solution) occurs at $\beta_{HB} = 11.8$. At this value of β a small modulation of the output signal occurs. Simultaneously, a dextro CP component of growing amplitude appears with the same frequency and 100% intensity modulation. The combination of both components results in a laser field with intensity and ellipticity oscillating around a mean value (which for the ellipticity is $+1$). Unlike this, the azi-

muth (whose value is arbitrary, as discussed in Sec. II) remains constant while the instantaneous value of the ellipticity is not equal to $+1$. Each time the ellipticity approaches this value, the azimuth jumps by $\pi/2$. Thus the trajectory of the laser-field polarization state is an arc symmetrically situated about the north pole along a meridian on the Poincaré sphere (Fig. 6, curve 1). This behavior remains up to a very large value of β ($\beta \sim 22$, Fig. 5), where the system evolves toward chaos. The (unstable) steady-state solutions disappear at $\beta = \beta_{PB}'' = 26.8$ (Fig. 4), but as shown in Fig. 5 in the present case the time-dependent solution remains until $\beta \sim 30$, where the inverse Hopf bifurcation affecting the off solution occurs. Approaching this value, the chaotic behavior progressively simplifies, transforming first into quasiperiodic and next into regular periodic behavior with modulation frequency defined by that of the Hopf bifurcation [17,18].

In contrast, as indicated above, if in the same conditions the coherent pumping is substituted by incoherent pumping, the behavior is "rotating linear" for any value of the upper-level incoherent pumping λ_0, although for $0.022 < \lambda_0 \lesssim 0.2$ a second solution exists which is also LP but its total intensity and azimuth strongly oscillate (chaotically for $\lambda_0 < 0.043$ and periodically for $\lambda_0 > 0.043$). The frequencies of its two CP components also oscillate slightly around the resonance value.

On the left-hand side of Fig. 4 (for instance, for $\gamma_b = 0.2$) the behavior is more sensitive to the value of γ_0. For $\gamma_0 = 1.0$ [Fig. 7(a)] the behavior is "rotating elliptical," i.e., the total intensity and ellipticity are constant in time and the azimuth rotates. This results in a trajectory on the Poincaré sphere, which surrounds it along the parallel in the north semisphere (Fig. 6, curve 2). The ellipticity is moderate (since the intensity of the one CP component is much larger than that of the other component), and these two CP components have slightly different frequencies. This solution is stable for any value of β and chaos never appears [Fig. 7(a)]. For $\gamma_0 = 0.5$ [Fig. 7(b)] the behavior is "rotating linear" just above the instability threshold $\beta_{HB} = 0.018$ (the time-modulated solution that arises at the HB loses very fast its stability and the system falls onto a rotating linear solution), rotating elliptical with time-dependent ellipticity for $0.8 \lesssim \beta < 21$, and chaotic for $\beta > 21$. The rotating elliptical behavior is different from that of Fig. 7(a), since now the
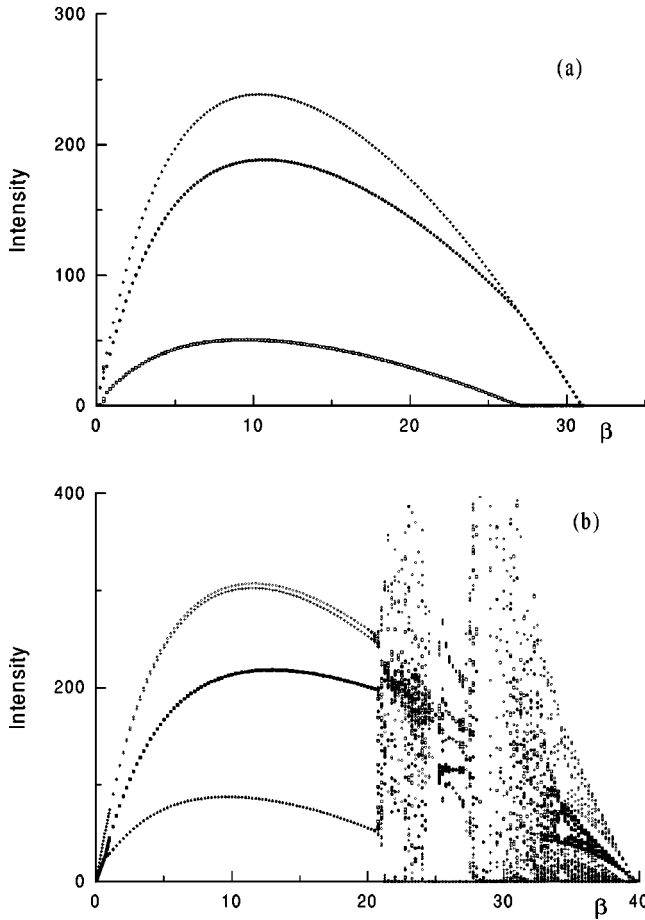
FIG. 7. The same as in Fig. 5 but for (a) $\gamma_0 = 1.0$, $\gamma_b = 0.2$ and $\gamma_0 = 0.5$, $\gamma_b = 0.2$.

FIG. 8. One-parameter diagrams of the field intensities (a) vs pump magnitude β for $\lambda_0 = 0$ and (b) vs incoherent pumping rate λ_0 for $\beta = 7 \times 10^{-4}$. $\gamma_0 = 0.01$, $\gamma_b = 0.2$. Other parameters, are the same as in Fig. 4. The notations are the same as in Fig. 5.

intensities of the two CP components strongly oscillate in time; the total intensity, however, is only weakly affected by this oscillation [Fig. 7(b)], which means that the two CP components oscillate in ''antiphase'' [23]. Superposition of these two CP antiphase oscillating solutions of slightly different frequencies produces time dependence of the ellipticity and continuous rotation of the polarization azimuth when trajectory alternatively visits the north and the south semispheres near equatorial circumference (Fig. 6, curve 3). Finally, for $\gamma_0 = 0.01$ [Fig. 8(a)] just above the instability threshold $\beta_{HB} = 0.84 \times 10^{-2}$ the emission is again rotating linear (as in Fig. 7(b) for small β], but now the system falls into chaos at quite a small value of β ($\beta \sim 0.06$). We interpret this appearance of chaos at low pumping as a consequence of the fact that in this case the population relaxation rates are very small and thus the system is well in the bad cavity limit; as it is well known in the standard Lorenz-Haken laser model, for these conditions the appearance of chaos is more likely. Nevertheless, the chaotic behavior that appears in our case is different from the Lorenz-Haken chaos since here the instability also affects the polarization degrees of freedom, as shown in Fig. 9, and there is a presence of coherent pumping. Clearly, the ellipticity and azimuth are also involved in the chaotic evolution [Figs. 9(b), and 9(c), and 9(e), and 9(f)]. The azimuth shows, in addition, $\pi/2$ sudden jumps each time the ellipticity reaches its extreme
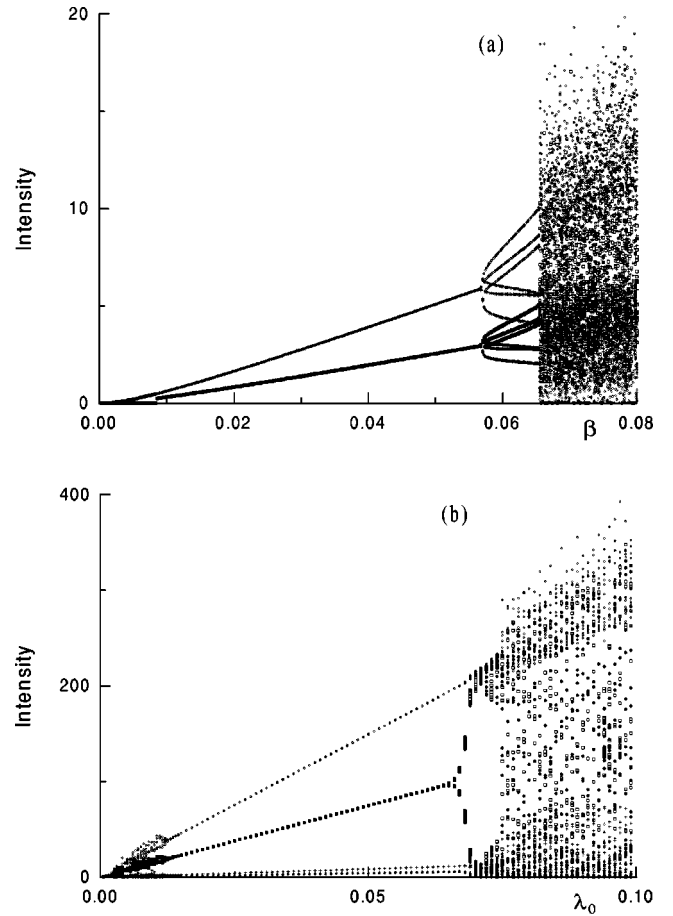
values $+1$ or -1. Figure 8(b) shows the same as in Fig. 8(a), but for an incoherently pumped laser. It can be seen that as the upper-level pumping rate λ_0 is increased, the behavior is not rotating linear in this case; the polarization is linear, but the azimuth, rather than continuously rotating, alternates at nearly constant evolution with sudden jumps of $\pi/2$ rad, at the same time that the intensity is deeply modulated in time. A common feature with the coherently pumped laser of Fig. 8(a), however, is that chaos also appears at relatively small pumping values, although the structure of the chaotic attractors has features different from those of the coherently pumped laser.

It is worth noting that in Figs. 5, 7(b), and 8, some small hysteresis effects have been found due to the coexistence of periodic or chaotic attractors (generalized bistability), but since the width of the hysteresis domains is small and the coexisting attractors involved are qualitatively similar, they have not been represented in the figures. Furthermore, the jumps between attractors often occur through long transients of metastable chaos.

Finally, Fig. 10 shows the dependence of the bifurcation thresholds on the cavity losses κ, for different values of γ_0 and γ_b (see figure caption). It is worth noting that the HB threshold (continuous line) is quite insensitive to the values
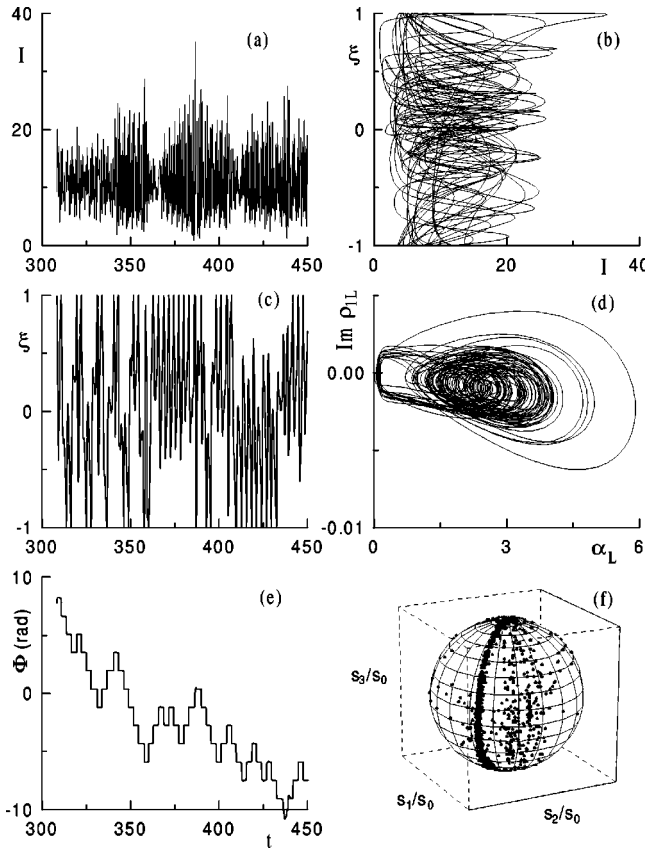
FIG. 9. Temporal evolution of the total laser field intensity I (a), the ellipticity parameter $\xi=(\alpha_L^2-\alpha_R^2)/I$ (c), and the polarization azimuth $\Phi=(\varphi_L-\varphi_R)/2$ (e). Phase projections of the chaotic attractor onto the (I,ξ) (b) and $(\alpha_L, \text{Im}\,\rho_{1L})$ (d) subspaces. (f) Trajectory of the chaotic field polarization state on the Poincaré sphere. Parameters are those as in Fig. 5 and $\beta=0.1$, $\gamma_0=0.01$, and $\gamma_b=0.2$.

FIG. 10. The meaning of all the curves is the same as in Fig. 4 but the thresholds are plotted in the subspace (β,κ) for $\gamma_\beta=0.9$, $\gamma_{Ph}=0.9$, $\gamma_J'=0.2$, $\gamma_C'=0.1$, $\gamma_0=0.5$, and $\gamma_b=0.8$ (1a). Other curves are plotted for $\gamma_0=0.25$ and different γ_b given in the figure. The other parameters are the same as in Fig. 4. Dots mark the codimensional-2 Takens-Boganov bifurcation. The corresponding magnitude of the losses (κ_{TB}) is depicted by the dashed-dotted-dotted line. The CP mode is stable ''on the left'' of the continuous curves.

of κ except for the important fact that below a certain threshold the HB instability disappears. This threshold value for κ is not far from the well known ''bad cavity'' condition $\kappa=\gamma_\parallel+\gamma_\perp$, but is not exactly that value, a fact that we interpret again as a result of the influence of the polarization degrees of freedom and coherent pumping. The vertical line indicates the value of the cavity losses where the HB and PB points affecting the off solution at large pumping values coincide, defining in this way a codimensional-2 Takens-Boganov bifurcation point.

V. CONCLUSIONS

In this work the results of analytical and numerical studies of an optically pumped $J''=1\rightarrow J=0\rightarrow J'=1$ isotropic cavity laser have been presented and compared with results from other laser systems. We have demonstrated that the behavior of such a system is dramatically different from that found in the case of a coherently pumped $J''=0\rightarrow J=1\rightarrow J'=0$ laser [7–10]. In contrast, it exhibits several features of an incoherently pumped $J=1\rightarrow J'=0$ [16] or $J=0\rightarrow J'=1$ isotropic cavity laser and also some features of a scalar three-level optically pumped laser [17,18].

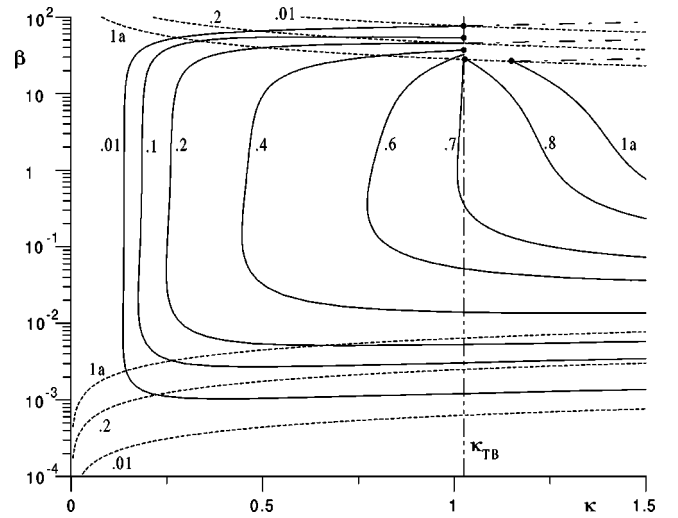In the coherently pumped $J''=0\rightarrow J=1\rightarrow J'=0$ laser, the behavior of the emitted field and its polarization state are almost fully controlled by the polarization state of the pumping field [8]. This is because in that system the pump field excites a certain atomic coherence in the upper level $J=1$ manifold, which generates a laser field with a well defined polarization state. This large gain anisotropy is not possible in our system since the upper level is a $J=0$ level. Thus, in our case gain anisotropy can only occur through the molecular dynamics in the $J''=1$ and $J'=1$ level manifolds (and their coupling with the fields) and through the two-photon (Raman) $J''=1\rightarrow J'=1$ pumping processes. A first consequence of this is that the polarization azimuth (along with global phase) explicitly disappears from the laser equations, which means that similar to the case of a conventional incoherently pumped $J=1\rightarrow J'=0$ [16] or $J=0\rightarrow J'=1$ isotropic cavity laser, the polarization azimuth in our system will be subject to diffusion driven by noise in spite of the presence of a strong and polarized pumping field.

A second consequence is that details of the molecular dynamics in the level manifold(s) are, as in the incoherently pumped $J=1\rightarrow J'=0$ or $J=0\rightarrow J'=1$ lasers, very important in determining the polarization dynamics. Unequal relaxation rates γ_J and γ_C (associated with the electric dipole and the magnetic quadrupole, respectively) of the lower level manifolds lead to either a preference for LP ($\gamma_C>\gamma_J$) or CP ($\gamma_C<\gamma_J$) emission in agreement with the maximum emission principle. That is, just above threshold the mode having larger intensity will be stable. Above the laser threshold a Hopf bifurcation occurs, which leads to a time-modulated regime that becomes immediately unstable and transforms into a regime with the presence of the two CP components of

the laser field. For the incoherently pumped $J=0 \to J'=1$ lasers, in most cases, this regime consists of LP emission with rotating azimuth, whereas for the coherently pumped laser it is more sensitive to the values of the molecular relaxation parameters and can lead to several regimes with different intensity and polarization dynamics (in particular, antiphase intensity dynamics and full polarization chaos).

Our laser system keeps also some inherent features of scalar optically pumped lasers. They are the following. First, there is an inverse pitchfork bifurcation at large pumping at which steady-state emission disappears, which is brought about by the strong pump-induced ac Stark splitting and shifting of the upper level out of the molecular resonance. Second, this ac Stark splitting at large pumping can generate modulated emission, which may last above the inverse pitchfork bifurcation, up to an inverse Hopf bifurcation of the off state. And third, these inverse pitchfork and Hopf bifurcations can collide defining a codimensional-2 Takens-Boganov bifurcation point.

All these results have been obtained in the limit of a perfectly isotropic cavity. Small cavity anisotropies could break the axial symmetry and thus could fix the polarization azimuth. The other polarization dynamics features described above, however, would in principle be only moderately affected by small cavity anisotropies, although it would be interesting to investigate this point in further detail.

From the results presented in this work we conclude that in laser systems involving atomic or molecular levels with low angular momentum quantum numbers, the dynamic behavior is very sensitive to the specific configurations that can be considered, and it can be difficult to draw general conclusions that might be applied to any system. These results

might stimulate experimental investigations similar to those of [11] which involve coherently pumped lasers with atomic amplifying media such as Ne (with the configurations pointed out in Sec. I), or further investigations with coherently pumped lasers. With respect to these last systems, at this moment our results (together with those of Refs. [7,8,10]) are not yet sufficient to understand the existing experimental results [13,14], which were obtained, as pointed out in Sec. I, with transitions involving angular momentum quantum numbers larger than those considered in the present work. In particular, we still do not understand why linear parallel polarization is generated in the 374 μm (^{15}NH$_3$) emission whereas linear orthogonal polarization is generated in the 81 μm (^{14}NH$_3$) and 153 μm (^{15}NH$_3$) emissions [15]. We think that, from the theoretical point of view, at least the configuration $J''=1 \to J=1 \to J'=1$ should be also considered (in spite of the larger mathematical difficulty of its study) in order to be able to draw general conclusions valid for cases of larger angular momenta. Also, from the experimental point of view, transitions with lower angular momenta could be investigated, provided the tunability domain of the pumping laser is increased, which can be achieved by modifying its cavity configuration [12].

APPENDIX: COEFFICIENTS AND SOME STEADY-STATE SOLUTIONS

1. Off solution

The coefficient B_0 in Eqs. (3) is

$$B_0 = \frac{\gamma_0 \lambda_2 \gamma_{2b} + 2\gamma_0 \lambda_2 \gamma_{2C} - 3\lambda_0 \gamma_{2b} \gamma_{2C}}{\gamma_{2C}(12\beta^2 \gamma_{2C} \gamma_{2b} + 8\beta^2 \gamma_0 \gamma_{2b} + 4\beta^2 \gamma_{2C} \gamma_0 + 3\gamma_{2C} \gamma_0 \gamma_{2b} \gamma_\beta)}.$$

The characteristic polynomial describing the stability conditions of the off solution—Eqs. (3)—is $X^4 + a_1 X^3 + a_2 X^2 + a_3 X + a_4 = 0$, where

$$a_1 = \gamma_{SPh} + \kappa + 1, \quad a_2 = (\rho_{1L} - \rho_0)g + (1 + \gamma_{SPh})\kappa + 2\beta^2 + \gamma_{SPh} + \gamma_{LPh}\gamma_{RPh},$$

$$a_3 = (2\kappa + \gamma_{SPh} - 2g\gamma_{2C}B_0)\beta^2 + \gamma_{SPh}(g\rho_{1L} - g\rho_0 + \kappa) + \gamma_{LPh}\gamma_{RPh}(1 + \kappa),$$

$$a_4 = \gamma_{SPh}(\kappa - g\gamma_{2C}B_0)\beta^2 + \gamma_{LPh}\gamma_{RPh}(g\rho_{1L} - g\rho_0 + \kappa).$$

Here for the sake of compactness we have introduced the notation $\gamma_{SPh} \equiv \gamma_{LPh} + \gamma_{RPh}$.

The pitchfork bifurcation threshold is given by the condition $a_4 = 0$, which leads to expression (4) with coefficients A_1, A_2, and A_3, given by

$$A_1 = \gamma_0 \gamma_{2C} + 3\gamma_{2b}\gamma_{2C} + 2\gamma_0 \gamma_{2b},$$

$$A_2 = -g(\gamma_{SPh}\gamma_0 + 4\gamma_{LPh}\gamma_{RPh})(2\gamma_{2C} + \gamma_{2b})\lambda_2 + 4\gamma_{LPh}\gamma_{RPh}A_1(\rho_{1L}g + \kappa)$$

$$-4\lambda_0 g\gamma_{LPh}\gamma_{RPh}(\gamma_{2C} + 2\gamma_{2b}) + 3\gamma_{2b}\gamma_{2C}\gamma_{SPh}(\lambda_0 g + \kappa\gamma_0 \gamma_\beta),$$

$$A_3 = g\,\gamma_0\rho_{1L} - \lambda_0 g + \kappa\,\gamma_0 .$$

Expression (4) is obtained assuming $|A_2| \gg A_3$, $A_2 < 0$, and $A_3 > 0$, which hold for lasers with large gain (g much larger than other characteristic constants of the system [2,17]), as is usually the case for optically pumped lasers.

2. Lasing solutions

Coefficients for the expressions for the intensities of the CP (5) and LP (6) modes are

$$A = -(4\beta^2\gamma_P + 3\gamma_b\gamma_C)(6\gamma_b\gamma_J\gamma_C + \gamma_M) + 9\gamma_b^2\gamma_C^2\gamma_J(16\beta^2 - 1),$$

$$B = \kappa(2\beta^2 + 1)(4\beta^2\gamma_P + 3\gamma_b\gamma_C) - 6g\beta^2(\gamma_b + 2\gamma_C),$$

$$C = 8\gamma_C^2(9\gamma_b^2 - 6\gamma_b - 1)\beta^4 - 32\gamma_b(\gamma_P - \gamma_b)\beta^2 - 3\gamma_b\gamma_C(3\gamma_b\gamma_C + 2\gamma_P),$$

$$\gamma_M = 3\gamma_b\gamma_C + \gamma_J\gamma_b + 2\gamma_J\gamma_C, \text{ and } \gamma_P = 3\gamma_b\gamma_C + 2\gamma_b + \gamma_C .$$

Populations of the left CP solution are

$$\rho_0 = \frac{1}{g}\,\frac{-6\alpha_L^4\kappa\gamma_b\gamma_C + 2\kappa[2\beta^2(3\gamma_C\gamma_b - 4\gamma_b - 2\gamma_C) - 3\gamma_C\gamma_b]\alpha_L^2 + 4g\beta^2(\gamma_b + 2\gamma_C)}{3\gamma_C\gamma_b(\alpha_L^2 + 1) + 4\beta^2\gamma_P},$$

$$\rho_{1L} = \alpha_L^2\kappa\,\frac{3\gamma_C\gamma_b + \gamma_J\gamma_b + 2\gamma_J\gamma_C}{3\gamma_C\gamma_J\gamma_b g}, \quad \rho_{1R} = \alpha_L^2\kappa\,\frac{-3\gamma_C\gamma_b + \gamma_J\gamma_b + 2\gamma_J\gamma_C}{3\gamma_C\gamma_J\gamma_b g}, \quad \rho_{10} = \alpha_L^2\kappa\,\frac{2\gamma_C'}{3\gamma_C\gamma_b g},$$

$$\rho_{2R} = \rho_{2L} = \frac{\gamma_C\alpha_L^2(g - 6\kappa\beta^2) + g(\gamma_C + 4\beta^2\gamma_C + 2\beta^2)}{3\gamma_C\gamma_b(\alpha_L^2 + 1) + 4\beta^2\gamma_P}\,\frac{\gamma_b + 2\gamma_C}{\gamma_C g}, \quad \rho_{20} = \frac{2\gamma_C'}{\gamma_b + 2\gamma_C}\rho_{2L} .$$

Populations of the LP solution are

$$\rho_0 = 2\kappa\,\frac{(8\gamma_b + 4\gamma_C - 6\gamma_C\gamma_b)\alpha_L^2 + 3\gamma_C\gamma_b(2\beta^2 + 1)}{9g\gamma_C\gamma_b}, \quad \rho_{1L} = \rho_{1R} = 2\alpha_L^2\kappa\,\frac{\gamma_b + 2\gamma_C}{3g\gamma_C\gamma_b}, \quad \rho_{10} = \frac{2\gamma_C'}{\gamma_b + 2\gamma_C}\rho_{1L},$$

$$\rho_{2L} = \rho_{2R} = -(\gamma_b + 2\gamma_C)\frac{4\kappa\gamma_P\alpha_L^2 + 3\gamma_C\gamma_b(2\kappa\beta^2 + \kappa - 3g)}{27g\gamma_C^2\gamma_b^2}, \quad \rho_{20} = \frac{2\gamma_C'}{\gamma_b + 2\gamma_C}\rho_{2L} .$$

---

[1] Y.I. Khanin, *Principles of Laser Dynamics* (Elsevier, Amsterdam, 1995).

[2] C.O. Weiss and R. Vilaseca, *Dynamics of Lasers* (VCH, Weinheim, 1991).

[3] H. Haken, *Light* (North-Holland, Amsterdam, 1985), Vol. 2.

[4] Special issue of Quant. Semiclassic. Opt. [**10**, Issue 1 (1998)] on *Polarization Effects in Lasers and Spectroscopy*, edited by N.B. Abraham and G.M. Stephan.

[5] Yu.P. Svirko and N.I. Zheludev, *Polarization of Light in Nonlinear Optics* (John Wiley & Sons, Chichester, 1998).

[6] L.A. Rivlin, Opt. Acoust. Rev. **1**, 125 (1990); L.A. Rivlin, Usp. Fiz. Nauk **167**, 309 (1997) [Sov. Phys. Usp. **40**, 291 (1997)].

[7] M. Arjona, R. Corbalán, F. Laguarta, J. Pujol, and R. Vilaseca, Phys. Rev. A **41**, 6559 (1990); R. Corbalán, R. Vilaseca, M. Arjona, J. Pujol, E. Roldán, and G.J. de Valcárcel, *ibid.* **48**, 1483 (1993); A. Kul'minskii, R. Vilaseca, and R. Corbalán, J. Mod. Opt. **42**, 2295 (1995).

[8] C. Serrat, R. Vilaseca, G.J. de Valcárcel, and E. Roldán, Phys. Rev. A **56**, 2327 (1997).

[9] C. Serrat, A. Kul'minskii, R. Vilaseca, and R. Corbalán, Opt. Lett. **20**, 1353 (1995); A. Kul'minskii, R. Vilaseca, and R. Corbalán, *ibid.* **20**, 2390 (1995).

[10] R. Vilaseca, C. Serrat, A. Kul'minskii, G.J. de Valcárcel, and E. Roldán, Quantum Semiclassic. Opt. **10**, 37 (1998).

[11] P.J. Manson, D.M. Warrington, N.L. Moise, and W.J. Sandle, Quantum Semiclassic. Opt. **10**, 157 (1998).

[12] N. G. Douglas, *Millimetre and Submillimetre Wavelength Lasers* (Springer, Berlin, 1989).

[13] C.O. Weiss and J. Brock, Phys. Rev. Lett. **57**, 2804 (1986); C.O. Weiss, N.B. Abraham, and U. Hubner, *ibid.* **61**, 1587 (1988); U. Hubner, N.B. Abraham, and C.O. Weiss, Phys. Rev. A **40**, 6354 (1989).

[14] D.Y. Tang, M.Y. Li, J.T. Malos, N.R. Heckenberg, and C.O. Weiss, Phys. Rev. A **52**, 717 (1995); D.Y. Tang and C.O. Weiss, *ibid.* **49**, 1296 (1994); D.Y. Tang, M.Y. Li, and C.O. Weiss, *ibid.* **46**, 676 (1992); *ibid.* **44**, 7597 (1991).

[15] See, for instance, the review paper E. Roldán *et al.*, Quantum Semiclassic. Opt. **9**, R1 (1997).

[16] N.B. Abraham, E. Arimondo, and M. San Miguel, Opt. Commun. **117**, 344 (1995); **117**, 244 (1995); M.D. Matlin, R.S. Gioggia, N.B. Abraham, P. Glorieux, and T. Crawford, *ibid.* **120**, 204 (1995); N.B. Abraham, M.D. Matlin, and R.S. Gioggia, Phys. Rev. A **53**, 3514 (1996).

[17] J.V. Moloney, J.S. Uppal, and R.G. Harrison, Phys. Rev. Lett. **59**, 2868 (1987); J.S. Uppal, R.G. Harrison, and J.V. Moloney, Phys. Rev. A **36**, 4823 (1987).

[18] W. Forysiak, R.G. Harrison, and J.V. Moloney, Phys. Rev. A **39**, 421 (1989); W. Forysiak, J.V. Moloney, and R.G. Harrison, Physica D **53**, 162 (1991).

[19] D. Lenstra, Phys. Rep. **59**, 299 (1980).

[20] J.R. Tredicce, F.T. Arecchi, G.L. Lippi, and G.P. Puccioni, J. Opt. Soc. Am. B **2**, 173 (1985); F.T. Arecchi, in *Optical Instabilities*, edited by R.W. Boyd, M.G. Raymer, and L.M. Narducci (Cambridge University Press, Cambridge, 1986), p. 183.

[21] G.P Agrawal and N.K. Kutta, *Long-wavelength Semiconductor Lasers*, 2nd ed. (Van Nostrand Reinhold, New York, 1993).

[22] J. Pujol, F. Laguarta, R. Vilaseca, and R. Corbalán, J. Opt. Soc. Am. B **5**, 1004 (1988).

[23] P. Mandel, *Theoretical Problems in Cavity Nonlinear Optics* (Cambridge University Press, Cambridge, 1997).